

RESEARCH ARTICLE

Fragility analysis of a multi-span continuous steel roadway bridge in Türkiye: A case study

Mehmet Fatih Yılmaz^{1*}, Abdülkadir Cüneyt Aydın²

- ¹ Ondokuz Mayıs University, Department of Civil Engineering, Samsun, Türkiye
- ² Atatürk University, Department of Civil Engineering, Erzurum, Türkiye

Article History

Received 10 August 2023 Accepted 13 September 2023

Keywords

Fragility curve
Bridge
Steel
Probability
Seismic performance
Damage
Time history

Abstract

One of the most widely utilized methods for determining seismic performance and allowing additional study is fragility analysis. The fragility curve, which is typically characterized by two-parameter log-normal distribution functions, depicts the probability of bridge components exceeding a certain damage limit. This study examines the fragility analysis of a multi-span continuous (MSC) steel roadway bridge in Türkiye. The probabilistic seismic demand model (PSDMs) is illustrated by conducting many time history analyses (THA). The nonlinear analyses are conducted for sixty earthquakes. Logarithmic regression analyses and fragility curves were derived for varying intensity measures (IM) in terms of efficiency. Monte Carlo analysis was used to derive the system fragility curve of the bridge. The PGA and ASI are the most proper intensity measure for the fragility curve of the bridge. Moreover, the slight damage can be visualized with a higher probability for the small intensity measure that even mild earthquake motion can cause some slight damage on the bridge but after slight damage bridge has further capacity until the collapse damage is visualized.

1. Introduction

Türkiye is situated in a seismically very active region and has experienced many devastating seismic events[1–6]. There has been significant damage to both bridges and buildings. Damage to the bridge not only causes huge retrofitting costs but also affects the ability to reach hazard areas, prevents vehicular access to hospitals, and causes important economic losses. As a result, numerous studies have concentrated on the earthquake performance of bridges. Earthquake loads on bridges were first taken into account in Japan in 1926 after the 1923 Kanto earthquake with a very simple approach. However, it was only possible after the 1970s for earthquake loads to be included in regulations in America and Europe. In Türkiye, there isn't private specification for the seismic design of the bridge so the American and European specifications are used. Therefore, road and railway bridges built before the 1970s have been designed without considering seismic loads and are under high seismic risk. Fragility analysis is a famous analyses tools that quickly and reliably estimated the earthquake performance of a single bridge or bridge network. Fragility is described as the likelihood of exceeding a certain limit under seismic occasions of structural or non-structural

eISSN 2630-5763 © 2023 Authors. Publishing services by golden light publishing®.

^{*} Corresponding author (<u>mehmetfatih.yilmaz@omu.edu.tr</u>)

components. There are traditionally three different methods used for deriving fragility curves: empirical, experimental, and analytical [7–9]. Empirical and experimental fragility curves are derived using past earthquake damage reports determined by experts and experimental study. For many structures, deriving empirical and experimental fragility curves is not possible for economic reasons and a lack of seismic damage reports. An analytical fragility curve can be derived using linear or nonlinear analyses. The most frequent analysis methods used to produce fragility curves are nonlinear time history analysis, incremental dynamic analysis, and capacity spectrum analysis [10–17]. A fragility curve is commonly expressed as a two-parameter (mean values and dispersion) log-normal distribution function[17]. These two parameters are both calculated depending on analytical results and experimental and empirical data.

A fragility curve allows the engineer to ascertain the damage probability of the structure under a seismic event. This very important knowledge is used in the different risk analyses and cost calculations and helps inform maintenance and repair decisions and many other studies. Damage to the bridge after a seismic event is calculated using a fragility curve. Also, it is studied whether or not road transportation to all hospitals in Istanbul can be sustained. Traffic intensity after the seismic event and the economical maintenance and repair period is calculated [18]. The fragility curve of the bridge might be derived for a specific bridge or for a bridge group that has similar seismic behavior [19–21]. Deriving the fragility curve for groups of bridges allows engineers to make a quick assessment of a particular group of bridges. However, grouping bridges is a very complicated activity because all specific bridges have important differences between them. Analyzing covariance of probabilistic seismic demand of bridges is used to classify bridges and identify a proper sample for fragility analysis and reduce the number of sampled bridges required to give reliable results [22].

Sustainability of the bridges system has essential importance for the transportation system. Any reduction of traffic flow because of maintenance activities and repairmen of bridges affect a growing economy in many direct and indirect ways [23]. Therefore, deriving a fragility curve becomes very important to reduce the seismic risk so as to allow the country to continue its development. The cost of retrofitting a damaged bridge after the seismic event can be determined using a cost-effective fragility curve [24]. The economic losses caused by a seismic event can be calculated easily. On the other hand, the amount of traffic is changes day by day, and overloaded trucks using the bridge call into question the old bridge's capacity to withstand these loads. The effects of the truck-bridge interaction on the fragility curve are investigated by conducting a finite element analysis, assuming the truck only as a mass and assuming the truck with mass and spring [22]. Moreover, natural hazards such as floods, hurricanes, and tsunamis also cause significant damage to the bridge. To predict this damage, some effort has been expended to derive a multi-hazard fragility curve considering both seismic and flood hazards [25, 26].

Fragility analysis of a multi span continuous steel roadway bridge in Türkiye is carried out. Real earthquake records used in the past studies are selected [9]. Nonlinear time-history analyses are conducted. A probabilistic seismic demand model of the bridge components is obtained using IM and demands. The efficiency of IM parameters is evaluated. The bridge components' fragility curves are derived. A Monte Carlo simulation with a sample was conducted to figure out the system fragility curve.

2. Analytical method and simulation

Fragility analyses are used accurately predict the earthquake performance of structural and non-structural components. The conditional probability of demand (EDP) corresponding to capacity (C) for a particular intensity measure (IM) value is defined as a fragility curve [27],

$$Fragility = P[EDP \ge C|IM] \tag{1}$$

where P[...] shows the probability of exceedance, EDP shows the engineering demand parameter, C shows the capacity of structure of structural components and IM shows the ground motion intensity measure. The

structural demand and capacity are determined using Non-linear Time History Analysis (NTHA), and PSDMs are developed.

2.1. Design stages for flexural strengthening

PSDM identifies the seismic demand of a structure or non-structural component in approximately one IM [28]

$$P[EDP \ge d|IM] = 1 - \Phi\left(\frac{\ln(d) - \ln(E\widehat{D}P)}{\beta_{EDP|IM}}\right)$$
 (2)

A power model is used to calculate the median EDP

$$E\widehat{D}P = aIM^b \tag{3}$$

or the logarithm model

$$ln(EDP) = ln(a) + b \times ln(IM) \tag{4}$$

where a and b are two-parameter of regression analysis, Φ is the standard cumulative normal distribution function, $E\widehat{D}P$ is the median engineering demand, d is damage limit state and $\beta_{EDP|IM}$ (dispersion) is the standard deviation of regression analysis [29],

$$\beta_{EDP|IM} \cong \sqrt{\frac{\sum (\ln(d_i) - \ln(aIM^b)^2}{N - 2}}$$
 (5)

2.2. Component and system fragility

Fragility curves are derived for each bridge components to determine the seismic behavior separately. With the help of the component fragility curve, the weakest bridge component can be determined easily, and any maintenance or additional investigation activity can be planned with the help of this valuable information. Nonlinear time-history analyses are utilized to calculate the structural demand relating to the ground motion IM, and component damage limits are computed individually to create the fragility curve.

Four damage states are determined for each bridge component. However, the system fragility curve of the bridge should be expressed with one curve that represents all the probability of exceeding of bridge component fragility curve. The unions of probabilities of each bridge component are defined as the bridge fragility curve for the damage state [30].

$$P[Fail_{system}] = \bigcup_{i=1}^{n} P[Fail_{component-i}]$$
(6)

To obtain the union probabilities of the component fragility curve a joint probability density function is derived with the help of Monte-Carlo simulation. One million samples are simulated considering the correlation between the component fragility curve and bridge probability is determined using the Eq. (6).

3. Case study

The Mahmutçavuş bridge is located 400 kilometers from the Pasinler, Oltu, Narman National Roadway on the Kışla Village Roadway. The bridge is a typical example of a multi-span continuous composite highway bridge. The bridge has two 10 m long spans at the initial and last and three 12 m long spans in the middle. The bridge's overall length is 56 meters, and its overall width is 5.4 meters. The bridge was built in 1961 and is still in use today. Abutments support the superstructure at the beginning and end, and steel piers in the

middle. The bridge's superstructure is made of steel and concrete composite sections, with elastomeric bearings on the middle piers and the abutments. Each pier includes four columns formed by welding two IPN 240 sections together. The bent beam has a width of 52 cm and a height of 58 cm. The slap measures 25 centimeters thick. Fig. 1 illustrates a general view of the bridge, while Fig. 2 displays a section view of the bridge. The bridge's superstructure consists of a 5 IPN360 steel beam and a concrete slab. The superstructure is continuous across the pier, with a moment release and expansion in the third span. The bridge crosses the Norman Stream, and the river's level is fluctuating. In the winter, only one bridge's pier is submerged, but all the bridge's piers are submerged in the spring and summer. The total height of the piers is 4 m. However, due to dirt deposition in the river, it is assumed that almost half of the piers are buried. This study does not take into account soil-structure interactions.

4. Mathematical modeling and simulation

4.1. Ground motion

With the help of the developing technology, the assumptions used in determining the earthquake loads have started to be determined in more realistic ways. In the specification before 2018, 4 different earthquake zones were defined and earthquake spectra were determined according to these 4 zones and site conditions.

After [31]Türkiye building seismic code was published, earthquake hazard maps become available and seismic load and spectra start to be determined in a site-specific way considering the coordinate of the building. Besides, non-linear analysis approaches were included in the design, and performance-based design methods were developed. These developments are desired to be included in the new specification prepared for Turkish seismic bridge design [32].

Three methods are encountered in the literature in deriving fragility curve with the help of NTHA. These are cloud, stripe and incremental dynamic analysis (IDA) [33, 34] Cloud method includes selecting different real earthquake data and using these data without scaling.

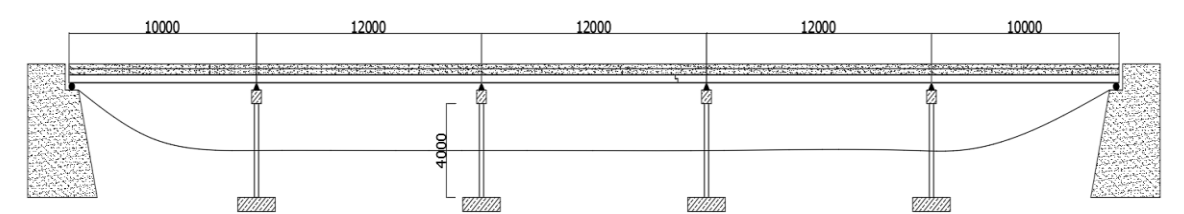


Fig. 1. MSC composite bridge from the side

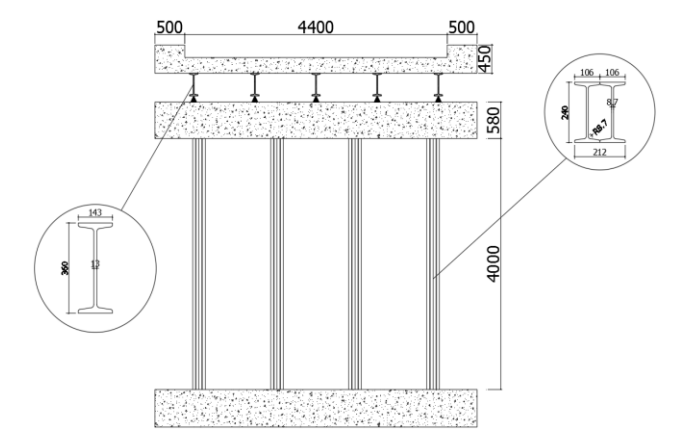


Fig. 2. MSC composite bridge in section

Although there is no accepted approach in selecting earthquake records in obtaining fragility curves, the main purpose of selecting records is to obtain many different earthquake forces in which different damage situations can be observed in bridges. If the selected earthquakes records consist of records with similar characteristics, the damage occurring in the bridges will be similar, so a limited number of similar properties will be observed and the desired data will not be obtained in the analysis results.

Random selection of earthquake data is applied considering the difference in terms of soil types, moment magnitude, PGAs, and central distances. The distribution of moment magnitude with a center distance is displayed in Fig. 3. The unscaled earthquake data were used for the time history analysis.

Fragility curve derived considering the different uncertainties on the structure as: capacities and loads. The most devastating of them is seismic loads. In these studies clouds approach is used to simulate the uncertainties of the seismic loads which is randomly select the real earthquake records and include the important uncertainties about the seismic loads. These are the strongest part of the cloud approach comparing with the static pushover and IDA. Because scaling the real earthquake data changes the characteristic properties of the earthquake records and sometimes create an earthquake record which is not possible to visualized in the real time. On the other hand static pushover analysis include many assumption to simplify the nonlinear analysis. Therefore cloud analysis has important advantages on simulating the uncertainties of the earthquake loads.

4.2. Analytical bridge models

SAP2000 finite element software is used to create a FE model of the bridge based on site inspection and measurement. Because of the bridge's construction date, there is no known architectural drawing or design project. As a result, all sections and lengths are measured on the site, and the bridge's FE model is constructed. The piers are represented by two-node beam elements, while four-node shell components represent the concrete slabs. Bridge abutments are not modeled and are considered to be fixed in these studies. Nonlinear link elements are used to model supports. The friction coefficient between the bearing and the support is computed and modeled using a friction link in the same way as it is for the elastomer pad. For small, moderate, large, and collapse damage states, the bearing's damage limit states are indicated by fractures in the pier, prying of the bearing and severe deformation in the anchor bolt, toppling or sliding of the bearing, and falling from the seat [35]. Fig. 4 depicts a 3D FE model of the bridge, whereas Fig. 5 depicts an actual photograph of the bridge.

Hysteresis behavior of elastomer bearings is determined considered by [35]. Nielson (2005) used testing data conducted by Mander et all, (1996) [36] and updated the information with the help of the expert report prepared after the earthquake and visualized damaged on bridge bearing in the US.

Earthquake Data Distribution

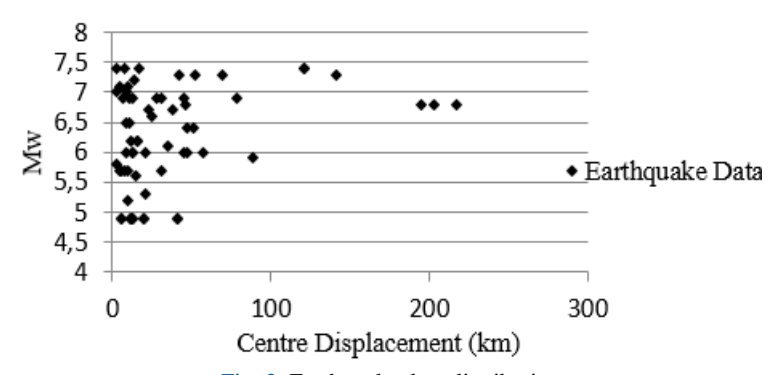


Fig. 3. Earthquake data distribution

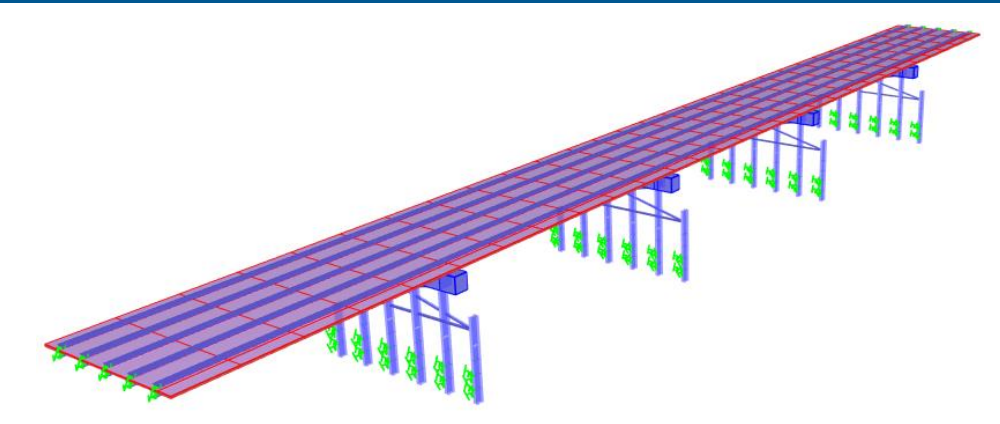


Fig. 4. Finite model view of MSC steel road bridge



Fig. 5. Picture of bridge

Material parameters are gathered from prior related literature because there is no specimen testing for this MSC bridge. Larsson and Lagerqvist [37] demonstrate that the material properties of existing steel bridges can be determined based on the years of construction by conducting experimental material tests on steel bridges in Europe. Yield and ultimate strengths for European railway and road bridges are $f_y = 220 \, MPa$ MPa and $f_u = 220 \, MPa$, respectively [37]. This study evaluates both the material and P- Δ large displacement behavior of bridges. Material nonlinearity is defined by PMM plastic hinges concentrated at the end of the piers and M2-M3 hinges concentrated at the ends and middle of the steel superstructure beam.

5. Discussion on intensity measures and demand models

5.1. Discussion on intensity measures

Fragility curves are traditionally derived considering only one IM parameter and the uncertainties mostly depend on the IMs. The optimum selection of the IM parameter helps to reduce the uncertainties of the fragility curve and determining damage probability more accurately. There are many different IM parameters are existed in the literature, and 9 of the most used are selected for this study as shown in Table 1. The selected IM parameters are compared in terms of practicality, efficiency, and proficiency.

The PGA, PGV, $S_{a-0.2s}$, and $S_{a-0.1s}$ IMs are parameters related to the vector characteristics of ground motion, such as spectral acceleration and displacement. I_A, I_V , CAV, CAD, and ASI. IMs are related to ground motion energy [38–42].

Practically express the correlation between IM and structural demand. Enlarging the correlation as well increases the practicalities and decreases the dispersion and uncertainties. b parameter determined by regression analysis of PSDM besides declares the correlation between IM and structural demand, and

practicality is expressed by b parameter. The higher values of b point to the more practical IM parameter. Dispersion expresses the demand alteration for the selected IM and describes the efficiency of the IM parameter. the smaller dispersion decreases the uncertainties and implies the more efficient IM parameter. Proficiency is determined as a parameter both include the effect of practicality and efficiency. To decrease the uncertainties the engineer looking for small dispersion and higher practicalities. Proficiency is expressed as the ratio of these parameters and the smaller examined for more accurate IM parameters [27].

$$\zeta = \frac{\beta_{EDP|IM}}{h} \tag{7}$$

Table 1. Intensity measures (IMs)

IM	Description	Units	Definition
PGA	Peak ground acceleration	g	$PGA = max \big \ddot{u}_g(t) \big $
PGV	Peak ground velocity	cm/s	$PGV = max \big \dot{u}_g(t) \big $
$S_{ ext{a-0.2s}}$	Spectral acceleration at 0.2s	g	$S_a(T_i) = w_i^2 S_d(T_i)$
$S_{ ext{a-0.1s}}$	Spectral acceleration at 1s	g	$S_a(T_i) = w_i^2 S_d(T_i)$
I_A	Area intensity	cm/s	$I_A = \frac{\pi}{2g} \int_0^{T_d} \left[\ddot{u}_g(t) \right] dt$
Iv	Velocity intensity	cm	$I_v = \frac{1}{PGV} \int_0^{T_d} [\dot{u}_g(t)] dt$
CAV	Cumulative absolute velocity	cm/s	$CAV = \int_0^{T_d} [\ddot{u}_g(t)] dt$
CAD	Cumulative absolute displacement	cm	$CAD = \int_0^{T_d} [\dot{u}_g(t)] dt$
ASI	Acceleration spectrum intensity	cm/s	$ASI = \int_{T_i}^{T_f} SA(T_i) dT$

Table 2. Comparisons between demand models and intensity measures

	C	olumn Rotatio	on	Pinned 1	Bearing Long	gitudinal	Sliding Bearing Longitudinal				
	b	$eta_{EDP IM}$	ζ	b	$eta_{EDP IM}$	ζ	b	$eta_{EDP IM}$	ζ		
IM	2.06	2.49	1.21	1.39	3.33	2.39	1.84	2.47	1.34		
PGA	2.08	2.45	1.18	1.53	3.26	2.14	2.24	2.05	0.92		
PGV	1.78	2.62	1.47	1.18	3.39	2.87	1.59	2.56	1.61		
$S_{a-0.2s}$	1.70	2.52	1.48	1.34	3.24	2.42	1.81	2.18	1.21		
$S_{ ext{a-0.1s}}$	1.22	2.37	1.95	0.89	3.23	3.61	1.21	2.16	1.79		
I_{A}	0.93	2.94	3.16	0.70	3.47	4.95	1.32	2.40	1.81		
I_{V}	0.71	2.97	4.21	0.51	3.49	6.88	0.74	2.77	3.74		
CAV	0.79	2.85	3.59	0.57	3.44	6.00	0.87	2.57	2.95		
CAD	2.17	2.34	1.08	1.64	3.20	1.95	2.16	2.12	0.98		
ASI	2.06	2.49	1.21	1.39	3.33	2.39	1.84	2.47	1.34		

Table 2 has been developed according to the probabilistic seismic demand model. The parameter b and $\beta_{EDP|IM}$ are determined by regression analysis and ζ calculated using these two-parameter. Column Rotation, Pinned bearing longitudinal, and sliding bearing longitudinal direction are the most fragile component of bridge therefore in the selection of proper IM these three components are considered. Maximum b = 2.17, 1.64, and 2.24 for the column rotation, pinned bearing longitudinal and sliding bearing longitudinal, respectively. Greater correlation IMs are more practical because higher correlation PSDMs produce more accurate outcomes. Thus, ASI, ASI, and PGV are more practical for column rotation, pinned bearing longitudinal, and sliding bearing longitudinal displacement, respectively.

Minimum $\beta_{EDP|IM} = 2.34$, 3.20, and 2.05 for the column rotation pinned bearing longitudinal and sliding bearing longitudinal displacement, respectively. Smaller dispersion IMs are more efficient because smaller dispersion PSDM produces more appropriate results. As a consequence, ASI and PGV are more effective than other IM alternatives.

Minimum ζ = 1.08, 1.95, and 0.92 for the column rotation, pinned bearing longitudinal and sliding bearing longitudinal displacement, respectively. Modified dispersion shows the practicality and efficiency of IMs, with smaller values indicating a more robust correlation and less dispersion between IMs and EDPs. Thus, ASI, and PGV are more proficient than other alternatives for column rotation, pinned bearing longitudinal displacement, and sliding bearing longitudinal displacement, respectively. The results show that seismic acceleration mostly affects column rotation and seismic velocity mostly affects bearing displacement.

5.2. Probabilistic seismic demand models

PSDMs were constructed from the column rotation and pinned and sliding bearing longitudinal displacement. Seismic demands received from sixty nonlinear time history analyses are used to derive PSDMs. ASI is the proper IM for column rotation and PGV is the proper IM for sliding bearing displacements. PSDMs are obtained considering the proper IM. Fig. 6 shows PSDMs for column rotation. Bridge collapse appears for six of the sixty analyses, so extensive plastic rotation is received and presented in PSDMs. Extensive longitudinal displacements are obtained for the same seismic record for pinned bearing longitudinal displacement but in the sliding bearing longitudinal direction. Fig. 7 shows PSDMs for pinned bearing and sliding bearing.

5.3. Determining bridge damage and limit states

Classification of damage is also an essential step in determining the earthquake performance of the bridge. Many damage states depend on plastic rotation, plastic curvature, ductility, and lateral displacement, and in the classification of bridge damage, retrofitting time is considered. Retrofitting of similar damage is expected to consume a similar amount of time. Damage happens due to extreme events documented in the literature, with bridge elements being classified into four separate damage classifications, which are slight, moderate, large, and collapse. There are several bridges without taking seismic loads into account. As a result, several types of damage to the bridge have been seen during earthquake occurrences.

The 1978 Miyagi-ken-Oki and 2011 Great East Japan earthquakes revealed a lack of column rotation and shear capacity, as well as damage to bridge bearings and steel bracing [43].

Different earthquake disasters have also resulted in damage to steel columns, lateral bracing, and bearings [35, 44]. Engineers may observe bridge performance under real-world settings by exposing them to earthquakes. Based on data from prior earthquakes and experimental study, a variety of possible damage limit states for assessing bridge performance have been established in the literature. Considering the yield rotation ratios of bridge column damage indicated by Choi et al. (2004), rotation limits were used to calculate the four types of damage in the columns. (see Tab. 3) and the four bearing displacement limitations are shown in Tab. 4.

The yielding rotation of the beam and column are calculated using Eq 8. Yield rotation for the beam is $\emptyset_y = 0.01512$ for the first and last span and $\emptyset_y = 0.01827$ for the middle spans, and yield rotation for the column is $\emptyset_y = 0.00414$.

$$\theta_{y} = \frac{W_{p} F_{y} l_{b}}{6E I_{b}} \tag{8}$$

where W_p plastic moment strength, F_y yielding strength, l_b length of the beam, E elastic modules of the beam, and I_b moment of inertia of the beam.

6. Fragility curve of the bridge

6.1. Fragility curve of bridge components

Bridge component damage limits for four damage states are illustrated in section 5.3. PSDMs of the bridge are derived using 60 real ground motion and NTHA. The cloud method is used in the selection of earthquake records. The fragility curve of bridge components is derived using PSDMs and damage limit states and is expressed as a two-parameter log-normal cumulative distribution function. PGA is used as an IM parameter because to be the most used IM in deriving bridge fragility curve and PGV is used in bivariate fragility analysis both for comparing and increasing the efficiency of the fragility curve. Fig. 8 show the flowchart of generating fragility curve and Fig. 9, Fig. 10, and Fig. 11 show the bridge components' fragility curves.

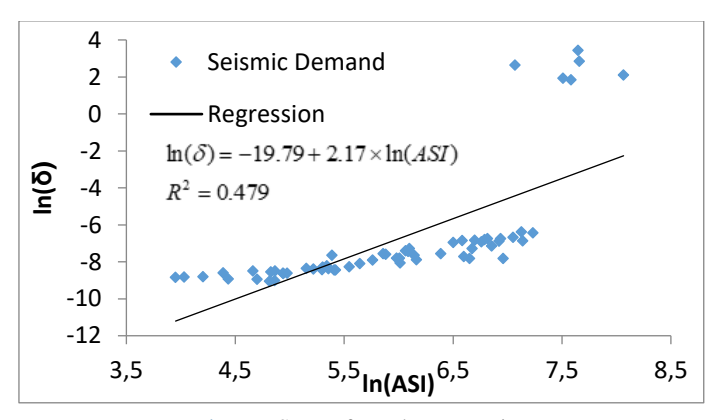
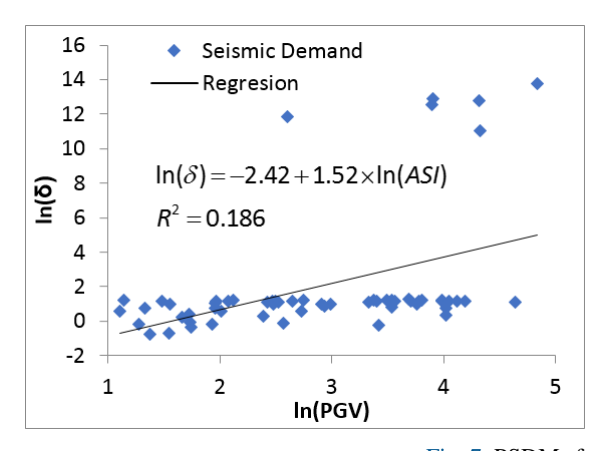


Fig. 6. PSDMs for column rotation



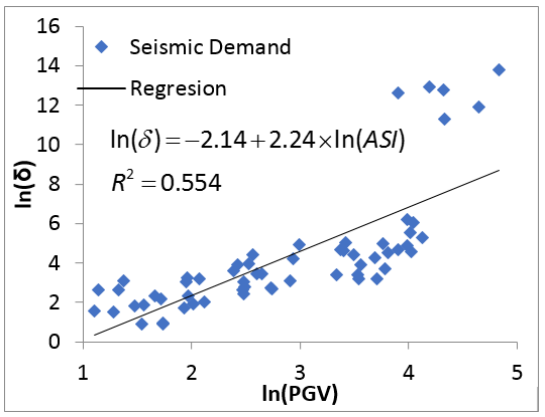


Fig. 7. PSDMs for column rotation

Table 3. Limitation of column damage

	Damage State			
	Slight	Moderate	Large	Complete
Column Rotation Ø	Ø _y	$2\phi_y$	$4\phi_y$	8Ø _y

Table 4. Bearing damage limit state [35]

	Damage State								
	Slight	Moderate	Large	Complete					
Pinned Bearing Longitudinal (mm)	28.9	104.2	136.1	186.6					
Pinned Bearing Transverse (mm)	28.8	90.9	142.2	195					
Sliding Bearing Longitudinal (mm)	28.9	104.2	136.1	186.6					
Sliding Bearing Transverse (mm)	28.8	90.9	142.2	195					

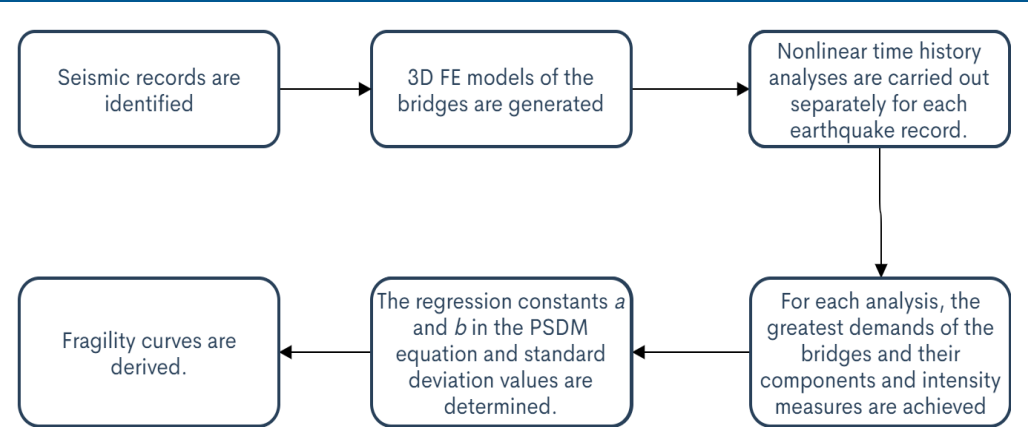


Fig. 8. Flowchart of generating fragility curve

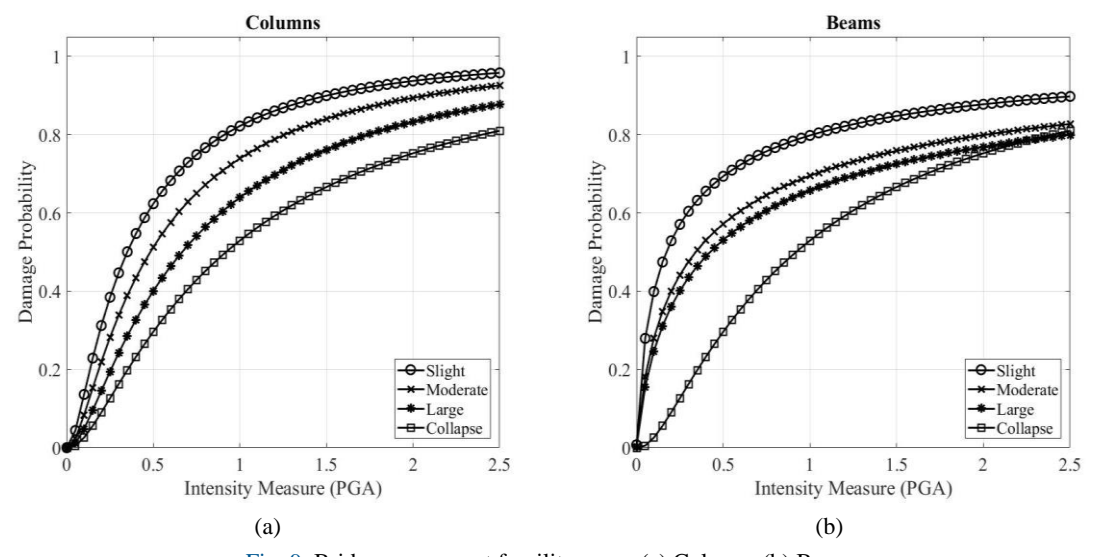


Fig. 9. Bridge component fragility curve (a) Column, (b) Beam

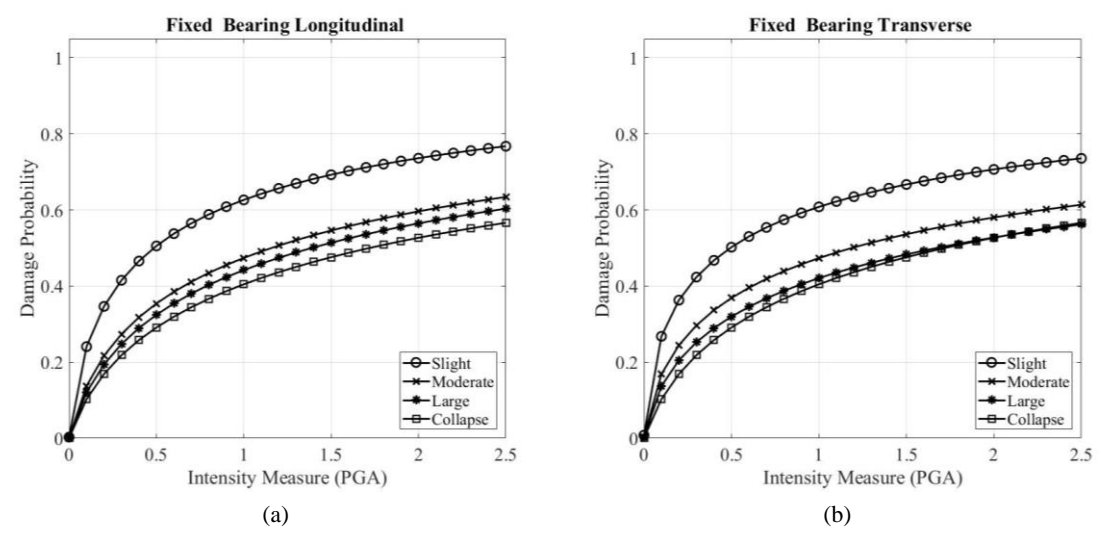


Fig. 10. Beam Bridge component fragility curve (a) Fixed bearing longitudinal direction (b) Fixed bearing transverse direction.

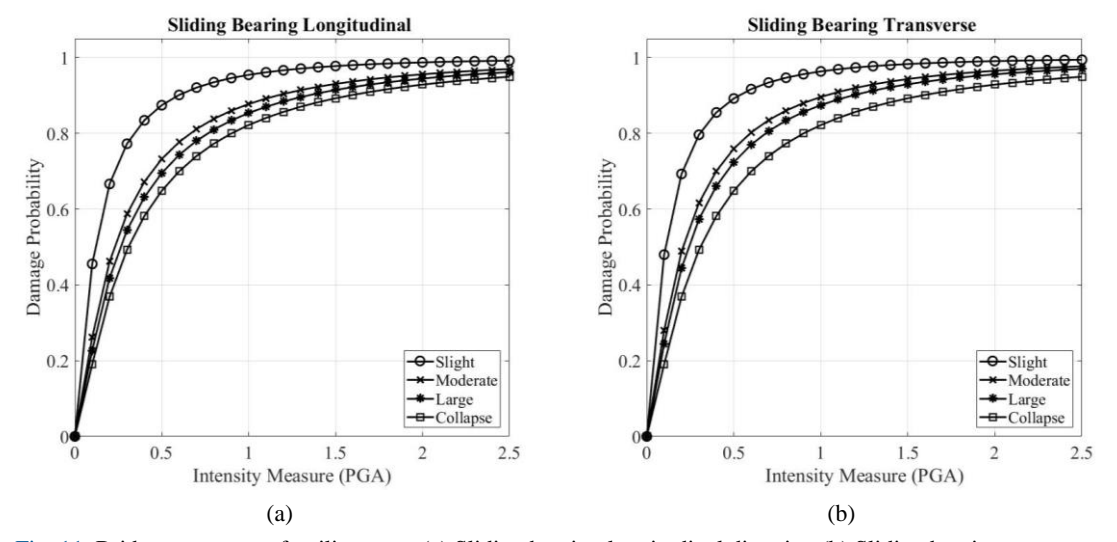


Fig. 11. Bridge component fragility curve (a) Sliding bearing longitudinal direction (b) Sliding bearing transverse direction

Component fragility curve shows that sliding bearing is the weakest component of the bridge and any retrofitting activities increase the capacities of sliding bearing have an important positive impact on the whole bridge systems earthquake performance. Because the dispersion of the fragility curve is high, there is some probability of damage visualized under lower IM.

6.2. Fragility curve of bridge components

Bridge system fragility curves are estimated with a joint probabilistic seismic demand model (JPSDM) considering each damage limit. Demands for each component are simulated using Monte Carlo simulation (one million samples) and system fragility curves are derived from Eq. (6).

To verify the system fragility curve upper and lower bounds are calculated with Eq. (9).

$$\max_{i=1}^{n} [P(F_i)] \le P(F_{system}) \le 1 - \prod_{i=1}^{m} [1 - P(F_i)]$$
(9)

where $P(F_i)$ is the probability of exceedance for component i, and $P(F_{system})$ is the failure probabil-ity of exceedance of the bridge system. The lower bound is calculated by taking maximum values of the probability of exceedance of each component and assume there is an exact correlation between this probability and provides a non-conservative result [30]. On the other hand, the upper bound theorem supposes no correlation between the probability of exceedance of component and gives the conserva-tive result. The system fragility curves are expected to be placed between these two bounds [30]. Fig. 12 shows the slight damage system fragility curve of the Mahmutçavuş bridge. The system fragility curve is significantly close to the lower bound. That indicates a strong relationship between the bridge system and the bridge component fragility curve. Fig. 13 shows the system fragility curve for four different damage states.

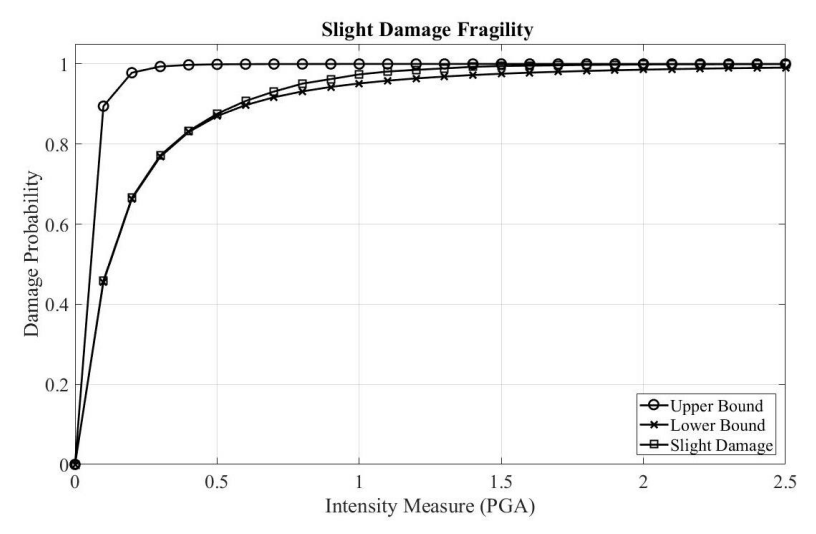


Fig. 12. Slight damage limits system fragility curve

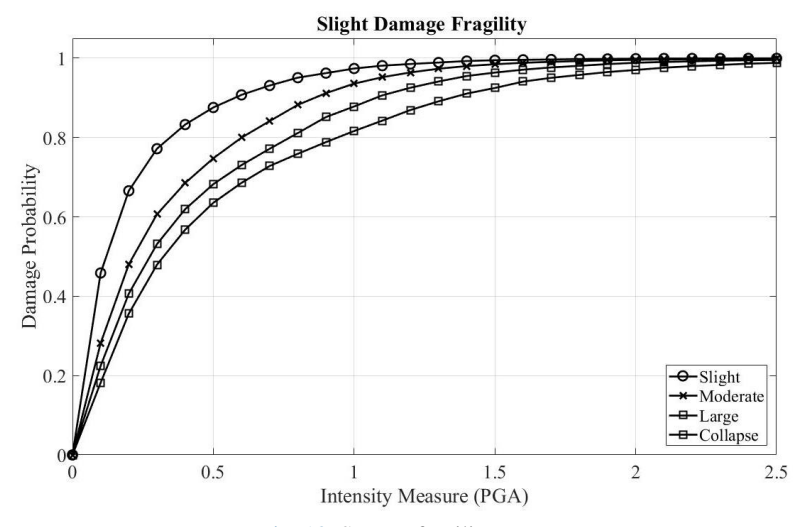


Fig. 13. System fragility curve

7. Bivariate fragility curve

Section 5 discusses the IM parameters and ascertains that the acceleration components of the earth-quake record are more effective for describing column and beam damage and the velocity components of the earthquake records are more effective for describing bearing damage. The classical definition of the fragility curve only allows the use of only a single IM parameter but using two IM parameters has increased the efficiency of the fragility curve and decreased dispersion [46]. Therefore, the surface fragility curve of the bridge was evaluated using PGA and PGV IM parameters together. A multi-variant cumulative log-normal distribution function is used to derive the surface fragility curve of the bridge and the correlation of two fragility curves is included in the analysis. Fig. 14 display the surface fragility curve of the bridge for four different damage states.

System fragility curves for both IMs are derived using a Monte Carlo simulation and two parameters (mean, dispersion) of the fragility curve are determined. Using these fragility curves and parameters, the cumulative joint probability matrix was derived using MATLAB. The new likelihood of transcending the damage limits now includes both the PGA and PGV effects. Therefore, this gives a more accurate result and allows these two parameters to be considered together while assessing this bridge.

8. Conclusions and comments

Earthquake assessment of a MSC steel, concrete road bridge is shown and explained. Sixty real earthquake records are selected and NTHA considering the Δ - δ effect and material nonlinearity is conducted. IM and the corresponding demand on bridge components are saved and PSDMs are derived. The fragility curve of bridge components is derived. The fragility curve of bridge components shows that sliding bearings are the weakest component of the bridge and are more fragile to damage than other components. Bridge columns are also fragile to seismic damage

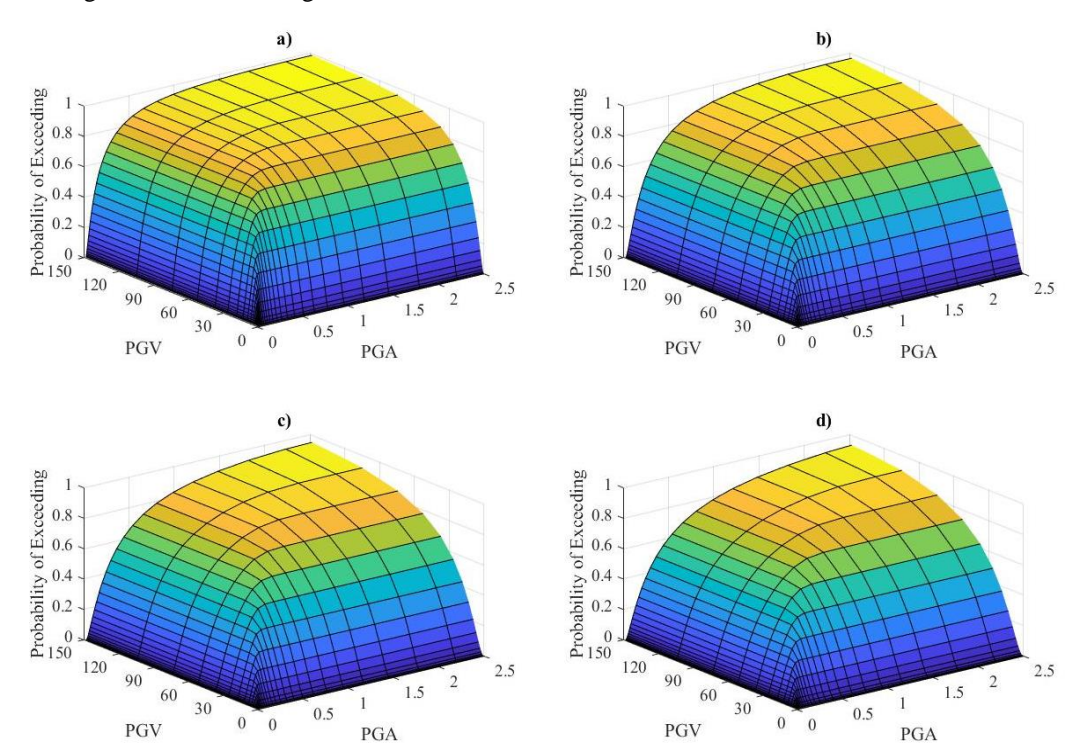


Fig. 14. Surface fragility curve of the bridge (a) Slight, (b) Moderate, (c) Extensive, (d) Collapse, damage state

Nine IM parameters used to derive fragility curves are selected and investigated in terms of efficiency. Because of the complexity of seismic events and nonlinear structural behavior and damage, expressing seismic demand with a single IM parameter is not easy. Therefore, further investigation is required to determine the most efficient IM parameters to derive more reliable PSDMs. IM parameters are investigated for three bridge components: column, pinned bearing, and sliding bearing. Acceleration parameters of the earthquake such as PGA and ASI give more efficient results for plastic rotation of the column but velocity parameters of the earthquake such as PGV give more efficient results for lateral displacement of bearings. The results show that the varying parameters for the earthquake behavior, cause different effects on the bridge components.

The system fragility curve of the bridge is estimated using a Monte Carlo simulation with 10⁶ sampling. Upper and lower bounds are derived to determine the system fragility curve. The system fragility curve gives a closer result to the lower bound, which means there is a reasonable correlation between the bridge systems and the bridge components' fragility curve. The 50% probability of exceeding damage limits is derived as 0.13g, 0.22g, 0.29g, and 0.34g for slight, moderate, large, and collapse damage states, respectively. The component fragility curves show that any retrofitting activities on the bridge components and sliding bearings result in significant improvements in the bridge system's fragility curve.

The surface fragility curve of the bridge system is derived from dealing with both the PGA and the PGV elements of the earthquake record. The PGA component is effective in determining column and beam damage and the PGV component is effective in determining bearing damage. The surface fragility curve includes elements of both PGA and PGV components, thus has less dispersion compared with the single component fragility curve and allows engineers to consider both IMs in seismic assessment of the bridge.

These studies express specific fragility curves of a case roadway bridge that was built-in 1961 and continue to give services. Although there are numerous studies derive fragility curves for brides, every bridge has their specific characteristics properties and generalization of the fragility curve are only a simplified methodology to allow bridge owners to determine bridge's performances with a fast and safe way. The obtained information is important for bridge owners in planning the maintenance and replacement activities for the bridge. According to the Türkiye Seismic Risk map's design earthquakes, PGA values are determined as 0.29g which is greater than slight and moderate damage to the bridge and equal to large damage's %50 probability of occurrence. The obtained fragility curves show that the bridge will suffer significant damage under a possible design earthquake.

Conflict of interests

The author(s) declared no potential conflicts of interest with respect to the research, authorship, and/or publication of this article.

Funding

This research received no external funding.

Data availability statement

No new data were created or analyzed in this study.

References

[1] Güllü H, Jaf HS (2016) Full 3D nonlinear time history analysis of dynamic soil–structure interaction for a historical masonry arch bridge. Environmental Earth Sciences 75(21):1-17.

[2] Güllü H, Pala M (2014) On the resonance effect by dynamic soil-structure interaction: A revelation study. Nat Hazards 72:827–847.

- [3] Güllü H, Karabekmez M (2017) Effect of near-fault and far-fault earthquakes on a historical masonry mosque through 3D dynamic soil-structure interaction. Engineering Structures 152:465–492.
- [4] Canakci H, Güllü H, Dwle MIK (2018) Effect of glass powder added grout for deep mixing of marginal sand with clay. Arabian Journal for Science and Engineering 43:1583–1595.
- [5] Ertürk E, Aykanat B, Altunışık AC, Arslan ME (2022) Seismic damage assessment based on site observation following the Düzce (Gölyaka) Earthquake (Mw = 5.9, November 23, 2022). Journal of Structural Engineering & Applied Mechanics 5:197–221
- Atmaca B, Arslan ME, Emiroğlu M, Altunişik AC, Adanur S, Demir A, Günaydin M, Kırtel O, Tatar T, Kahya V, Sunca F, Okur FY, Hacıefendioğlu K, Dok G, Öztürk H, Vural İ, Güleş O, Genç AF, Demirkaya E, Yurdakul M, Nas M, Akbulut YE, Baltacı A, Temel BA, Başağa HB, Sarıbıyık A, Şen F, Aykanat B, Öztürk İŞ, Navdar MB, Aydın F, Öntürk K, Utkucu M, Akgül T (2023) On the earthquake-related damages of civil engineering structures within the areas impacted by Kahramanmaraş Earthquakes. Journal of Structural Engineering & Applied Mechanics 6(2):98-116.
- [7] Gautam D (2017) On seismic vulnerability of highway bridges in Nepal: 1988 Udaypur Earthquake (MW 6.8) revisited. Soil Dynamics and Earthquake Engineering 99:168–171
- [8] Yazgan U (2015) Empirical seismic fragility assessment with explicit modeling of spatial ground motion variability. Engineering Structures 100:479–489.
- [9] Yilmaz MF, Çalayan B (2018) Seismic assessment of a multi-span steel railway bridge in Türkiye based on nonlinear time history. Natural Hazards and Earth System Sciences 18:231–240
- [10] Shinozuka M, Banerjee S, Kim S-H (2007) Statistical and Mechanistic Fragility Analysis of Concrete Bridges.
- [11] Bignell JL, LaFave JM, Wilkey JP, Hawkins NM (2004) Seismic Evaluation ff Vulnerable Highway Bridges with Wall Piers On Emergency Routes. In: 13th World Conference on Earthquake Engineering. Southern Illinois, ABD.
- [12] Kumar R, Gardoni P (2014) Effect of seismic degradation on the fragility of reinforced concrete bridges. Engineering Structures 79:267–275.
- [13] Kurian Sa, Deb SK, Dutta A (2006) Seismic Vulnerability Assessment of a Railway Overbridge Using Fragility Curves. In Proceeding of: 4th International Conference on Earthquake Engineering. Taipei, Taiwan.
- [14] Liolios A, Panetsos P, Hatzigeorgiou G, Radev S (2011) A numerical approach for obtaining fragility curves in seismic structural mechanics: A bridge case of Egnatia Motorway in northern Greece. Lect Notes Comput Sci (including Subser Lect Notes Artif Intell Lect Notes Bioinformatics) 6046 LNCS:477–485.
- [15] Mackie K, Stojadinovic B (2003) Seismic Demands for Performance-Based Design of Bridges.
- [16] Mackie K, Stojadinović B (2001) Probabilistic seismic demand model for california highway bridges. Journal of Bridge Engineering 6(6):468–481.
- [17] Shinozuka M, Feng MQ, Kim H, Kim SH (2000) Nonlinear static procedure for fragility curve development. Journal of Engineering Mechanics 126(12):1287–1295.
- [18] Bakioğlu G, Karaman H (2018) Accessibility of medical services following an earthquake: A case study of traffic and economic aspects affecting the Istanbul roadway. International Journal of Disaster Risk Reduction 31:403–418.
- [19] Stefanidou SP, Kappos AJ (2017) Methodology for the development of bridge-specific fragility curves. Earthquake Engineering & Structural Dynamics 46(1):73–93.
- [20] Stefanidou SP, Kappos AJ (2019) Bridge-specific fragility analysis: when is it really necessary? Bulletin of Earthquake Engineering 17, 2245-2280.
- [21] Zampieri P, Zanini MA, Faleschini F (2016) Derivation of analytical seismic fragility functions for common masonry bridge types: methodology and application to real cases. Engineering Failure Analysis 68:275–291.
- [22] Mangalathu S, Jeon JS, Padgett JE, DesRoches R (2016) ANCOVA-based grouping of bridge classes for seismic fragility assessment. Engineering Structures 123:379–394.
- [23] Kilanitis I, Sextos A (2019) Integrated seismic risk and resilience assessment of roadway networks in earthquake prone areas. Bulletin of Earthquake Engineering 17:181–210.
- [24] Seo J, Park H (2017) Probabilistic seismic restoration cost estimation for transportation infrastructure portfolios with an emphasis on curved steel I-girder bridges. Structural Safety 65:27-34.

- [25] Gehl P, Ayala DD (2016) Development of Bayesian Networks for the multi-hazard fragility assessment of bridge systems. Structural Safety 60:37–46.
- [26] Kocaman İ, Yılmaz M, Tosunoğlu F, Kazaz İ (2022) The behavior of the historical Çobandede Bridge under flood load. Journal of Structural Engineering & Applied Mechanics 5:249–263.
- [27] Padgett JE, Nielson BG, DesRoches R (2008) Selection of optimal intensity measures in probabilistic seismic demand models of highway bridge portfolios. Earthquake Engineering and Structural Dynamics 37:711–725.
- [28] Padgett JE, DesRoches R (2008) Methodology for the development of analytical fragility curves for retrofitted bridges. Earthquake Engineering and Structural Dynamics 37:1157–1174.
- [29] Siqueira GH, Sanda AS, Paultre P, Padgett JE (2014) Fragility curves for isolated bridges in Eastern Canada using experimental results. Engineering Structures 74:311–324.
- [30] Nielson BG, DesRoches R (2007) Seismic fragility methodology for highway bridges using a component level approach. Earthquake Engineering and Structural Dynamics 36:823–839.
- [31] TBEC (2018) Tukey Building Earthquake Code. Disaster and Emergency Management Presidency, Ankara, Tukey.
- [32] KGM (2019) Karayolu ve Demiryolu Köprü ve Viyadükleri Deprem Yönetmeliği Taslak Raporu.
- [33] Mackie KR, Stojadinovic B (2005) Comparison of Incremental Dynamic, Cloud and Stripe Methods for computing Probabilistic Seismic Demand Models. Structures Congress 171: 184.
- [34] Dolsek M (2009) Incremental dynamic analysis with consideration of modeling uncertainties. Earthquake Engineering and Structural Dynamics 38:805–825.
- [35] Nielson BG (2005) Analytical fragility curves for highway bridges in moderate seismic zones. Georgia Institute of Technology.
- [36] Mander J, Kim D, Chen S, Premus G (1996) Response of steel bridge bearings to the reversed cyclic loading.
- [37] Larsson T, Lagerqvist O (2009) Material properties of old steel bridges. Nord. Steel Constr. Conf.
- [38] Hsieh SY, Lee CT (2011) Empirical estimation of the newmark displacement from the arias intensity and critical acceleration. Engineering Geology 122:34–42.
- [39] Kayen RE, Mitchell JK (1997) Assessment of liquefaction potential during earthquakes by arias intensity. J Geotech Geoenvironmental Eng 123:1162–1174.
- [40] Mackie KR, Stojadinovic B (2004) Improving Probabilistic Seismic Demand Models Through Refined Intensity Measures. In Proceeding of: 13th World Conference on Earthquake Engineering. Vancouver, B.C., Canada.
- [41] Özgür A (2009) Fragility Based Seismic Vulnerability Assessment of Ordinary Highway Bridges in Türkiye. PhD Dissertation. Middle East Technical University.
- [42] Avşar Ö, Yakut A, Caner A (2011) Analytical Fragility Curves for Ordinary Highway Bridges in Türkiye. Earthquake Spectra 27:971–996.
- [43] Kawashima K (2012) Damage of bridges due to the 2011 great East Japan earthquake. Japan Association for Earthquake Engineering 12:319–338.
- [44] Kunnath SK, Erduran A, Chai YH, Yashinsky M (2008) Effect of vertical motions on seismic response of highway bridges. Journal of Bridge Engineering 13:282–290.
- [45] Choi E, DesRoches R, Nielson B (2004) Seismic fragility of typical bridges in moderate seismic zones. Engineering Structures 26:187–199.
- [46] Gehl P, Seyedi DM, Douglas J (2013) Vector-valued fragility functions for seismic risk evaluation. Bulletin of Earthquake Engineering 11:365–384.

Annex 1. Selected Earthquake Record

						Se	lected I	Earthqua	ke Rec	ord							
Earthquake	Date	Moment Magnitute	Record	PGA	Central Distance	Earthquake	Date	Moment Magnitute	Record	PGA	Central Distance	Earthquake	Date	Moment Magnitute	Record	PGA	Central Distance
		$(\mathbf{M}_{\mathrm{w}})$		(g)	(km)			$(\mathbf{M}_{\mathrm{w}})$		(g)	(km)			(M_w)		(g)	(km)
Anza (Horse Cany)	25.02.1980	4.9	AZF315	0.066	12.1	Parkfield	28.06.1966	5.6	C12320	0.0633	14.7	Borrego Mtn	09.04.1968	6.8	A-ELC180	0.13	46
Morgan Hill	24.04.1984	6.2	G01320	0.098	16.2	Morgan Hill	24.04.1984	6.2	GIL067	0.1144	16.2	Borrego Mtn	09.04.1968	6.8	A-PEL090	0.012	217.4
Coyote Lake	06.08.1979	5.7	G01320	0.132	9.3	Kocaeli	17.08.1999	7.4	ARC000	0.2188	17	Borrego Mtn	09.04.1968	6.8	A-TLI249	0.01	195
Landers	28.06.1992	7.3	GRN180	0.041	141.6	Morgan Hill	24.04.1984	6.2	G06090	0.292	11.8	Coyote Lake	06.08.1979	5.7	G02140	0.339	7.5
Landers	28.06.1992	7.3	ABY090	0.146	69.2	Coyote Lake	06.08.1979	5.8	G06230	0.4339	3.1	Coyote Lake	06.08.1979	5.7	G03050	0.272	6
Landers	28.06.1992	7.3	SIL000	0.05	51.7	Northridge	17.01.1994	6.7	ORR090	0.5683	22.6	Coyote Lake	06.08.1979	5.7	G04270	0.248	4.5
Landers	28.06.1992	7.3	29P000	0.08	42.2	Loma Prieta	18.10.1989	7.1	CLS000	0.6437	5.1	Coyote Lake	06.08.1979	5.7	HVR150	0.039	31.2
Loma Prieta	18.10.1989	6.9	G01090	0.473	11.2	Kobe	16.01.1995	6.9	KJM000	0.8213	6.9	Imperial Valley	15.10.1979	7	I-ELC180	0.313	8.3
Loma Prieta	18.10.1989	6.9	SGI360	0.06	30.6	Santa Barbara	13.08.1978	7.2	SBA222	0.203	14	Imperial Valley	15.10.1979	7	H-AEP045	0.327	8.5
Loma Prieta	18.10.1989	6.9	MCH000	0.073	44.8	Livemor	27.01.1980	7.4	LMO355	0.252	8	Imperial Valley	15.10.1979	7	H-BCR230	0.775	2.5
Loma Prieta	18.10.1989	6.9	PTB297	0.072	78.3	N. Palm Springs	08.07.1986	6	DSP000	0.331	8.2	Imperial Valley	15.10.1979	6.5	H-BRA315	0.22	8.5
Lytle Creek	12.09.1970	5.9	CSM095	0.071	88.6	N. Palm Springs	08.07.1986	6	FVR045	0.129	13	Imperial Valley	15.10.1979	6.5	H-CX0225	0.275	10.6
N. Palm Springs	08.07.1986	6	AZF225	0.099	20.6	Northridge	17.01.1994	6.7	TPF000	0.364	37.9	Hollister	28.11.1974	5.2	A-HCH271	0.177	10
N. Palm Springs	08.07.1986	6	ARM360	0.129	46.7	San Fernando	02.09.1971	6.6	ORR021	0.324	24.9	Cape Mendocino	25.04.1992	7.1	PET090	0.662	9.5
N. Palm Springs	08.07.1986	6	H02090	0.093	45.6	Whitter Narrows	10.01.1987	6	ALH180	0.333	13.2	Coalinga	02.05.1983	6.4	H-C05270	0.147	47.3
N. Palm Springs	08.07.1986	6	H02000	0.07	57.6	Kocaeli	17.08.1999	7.4	SKR090	0.376	3.1	Coalinga	02.05.1983	6.4	H-C08000	0.098	50.7
Whittier Narrows	01.10.1987	5.3	MTW000	0.123	20.4	Victoria, Mexica	09.06.1980	6.1	CPE045	0.62	34.8	Kern County	21.07.1952	7.4	Pas 180	0.051	120.5
Anza (Horse Cany)	25.02.1980	4.9	AZF225	0.065	12.1	Anza (Horse Cany)	25.02.1980	4.9	BAR225	0.047	40.6	Kern County	21.07.1952	7.4	PEL180	0.058	120.5
Anza (Horse Cany)	25.02.1980	4.9	PTF135	0.131	13	Anza (Horse Cany)	25.02.1980	4.9	RDA045	0.097	19.6	Loma Prieta	18.10.1989	6.9	HCH090	0.247	28.2
Anza (Horse Cany)	25.02.1980	4.9	TVY135	0.081	5.8	Borrego Mtn	09.04.1968	6.8	PAS270	0.09	203	Loma Prieta	18.10.1989	6.9	G02000	0.367	12.7